



Contents lists available at ScienceDirect

Journal of Biomechanics

journal homepage: www.elsevier.com/locate/jbiomech
www.JBiomech.com

Short communication

A database of lumbar spinal mechanical behavior for validation of spinal analytical models



Ian A.F. Stokes*, Mack Gardner-Morse

University of Vermont, Department of Orthopaedics and Rehabilitation, Burlington, VT 05405-0084, USA

ARTICLE INFO

Article history:

Accepted 28 January 2016

Keywords:

Spine
Lumbar spine
Stiffness
Preload
Frequency-dependence
Database

ABSTRACT

Data from two experimental studies with eight specimens each of spinal motion segments and/or intervertebral discs are presented in a form that can be used for comparison with finite element model predictions. The data include the effect of compressive preload (0, 250 and 500 N) with quasistatic cyclic loading (0.0115 Hz) and the effect of loading frequency (1, 0.1, 0.01 and 0.001 Hz) with a physiological compressive preload (mean 642 N). Specimens were tested with displacements in each of six degrees of freedom (three translations and three rotations) about defined anatomical axes. The three forces and three moments in the corresponding axis system were recorded during each test. Linearized stiffness matrices were calculated that could be used in multi-segmental biomechanical models of the spine and these matrices were analyzed to determine whether off-diagonal terms and symmetry assumptions should be included.

These databases of lumbar spinal mechanical behavior under physiological conditions quantify behaviors that should be present in finite element model simulations. The addition of more specimens to identify sources of variability associated with physical dimensions, degeneration, and other variables would be beneficial. Supplementary data provide the recorded data and Matlab[®] codes for reading files. Linearized stiffness matrices derived from the tests at different preloads revealed few significant unexpected off-diagonal terms and little evidence of significant matrix asymmetry.

© 2016 Elsevier Ltd. All rights reserved.

1. Introduction

Analytical models of the biomechanical function of the spine and spinal motion segments together with experimental studies provide understanding of *in vivo* spinal loading as well as the biomechanics of the intervertebral discs and motion segments. Finite element models have been used to gain understanding of elastic load-deformation behavior (Dreischarf et al., 2014; Weisse et al., 2012), time-dependent behavior (Castro et al., 2014; Galbusera et al., 2011a, 20011b; Schmidt et al., 2010; Schroeder et al., 2010) and insights into damage accumulation (Qasim et al., 2012), degeneration and transport of nutrients and metabolites (Natarajan et al., 2004; Schmidt et al., 2013). Models are also used to predict the behavior of surgical implants (Zhang and Teo, 2008), and in multi-segmental spine models to estimate *in vivo* spinal and muscular forces with each motion segment represented by a stiffness matrix or equivalent beam (Gardner-Morse and Stokes, 2004). While motion segment and disc models are becoming increasingly sophisticated by including complex elastic formulations, creep,

viscoelasticity and swelling behavior, there is a shortage of experimental data for validation of the complex nonlinear, time-dependent six-degree of freedom behavior of the spine. Although tissue properties have been extensively studied (e.g. Cloyd et al., 2007; O'Connell, Sen and Elliott, 2012; Wagnac et al., 2011), the structural behaviors of discs and motion segments including the neural arch and facet joints are not well documented.

The intervertebral disc is a complex avascular structure having nonlinear behavior in six degrees of freedom with stiffness that increases with axial compressive load (Gardner-Morse and Stokes, 2004), and with time dependent response (creep, hysteresis, etc.). The disc is commonly modeled as a biphasic tissue with fluid and solid phases, also sometimes including fixed charges responsible for swelling behavior and retention of fluid. The nonlinear elastic behavior is thought to result primarily from the cable-like nature of collagen fibers, and its time-dependent behavior resulting from both fluid-flow effects and solid phase viscoelasticity (Costi et al., 2008).

Motion segment behavior in multi-segmental analyses of spinal and trunk loading and stability can be represented efficiently by use of a continuum formulation such as a linearized stiffness matrix or 'equivalent' beam (Gardner-Morse and Stokes, 2004). Most of the available motion segment data are limited to axial

* Corresponding author. Tel.: +1 802 656 2250; fax: +1 802 656 4249.
E-mail address: ian.stokes@uvm.edu (I.A.F. Stokes).

compression stiffness and creep, and elastic behavior in the three principal angular degrees of freedom. The full linear stiffness matrix as required for equivalent structure representation comprises both diagonal and off-diagonal terms and matrix symmetry. Goel (1987) noted that certain forces or moments are associated with at least two displacements (in a flexibility experiment) and identified them as 'primary' and 'secondary'. For example, an anterior force would generally produce anterior shear (primary) as well as flexion (secondary) motion. Secondary motion is often also identified as 'coupling' behavior. Also, any misalignment of the applied force relative to structural symmetry axes of the specimen would produce additional out-of-plane motion. Here in the context of a stiffness experiment (applied displacements) we identify primary terms as the diagonal terms of the stiffness matrix, and secondary (expected) off-diagonal terms; also additional off-diagonal terms resulting from structural asymmetry or testing axis misalignment. In experimentally determined stiffness matrices, translational stiffness should be independent of the center of the axis system, but rotational stiffness terms would be axis-center dependent. (The inverse is the case for a flexibility matrix).

The purpose of this paper is to provide data for use in validation of analytical models or other analyses of the lumbar spine. Data were recorded from two sets of human lumbar motion segments (without posterior elements for the second set) in six degrees of freedom, under different axial preloads and with different loading frequencies. The data have previously been used to report stiffening by preload and representation of the motion segment as an 'equivalent' beam (Gardner-Morse and Stokes, 2004) and in a study of frequency-dependent apparent stiffness and hysteresis behavior under cyclic loading (Costi et al., 2008) with testing frequencies covering the range from quasistatic to walking.

Experimental data were also examined to identify significant off-diagonal terms in the derived linearized stiffness matrices and to determine their degree of symmetry. These matrices are symmetrical in a linear elastic structure, but experimentally have been found to be asymmetrical (Holsgrove et al., 2015) in porcine motion segments. Previously published experimentally derived

stiffness matrices using this database (Gardner-Morse and Stokes, 2004) assumed symmetry.

2. Methods

Data for the six-degrees of freedom behavior of human cadaveric motion segments were recorded using a 'hexapod' (Stewart platform) apparatus (Stokes et al., 2002). This computer-controlled apparatus has six linear actuators, six displacement transducers and a six-degree-of freedom load cell. It was programmed to impose each of the three principal displacements and three principal rotations in the motion segment's local axis system while the three principal forces and moments were recorded. Human motion segments were dissected from available human spines (thus a sample of convenience) that had been stored at -80°C . Each specimen was radiographed and no evidence of anatomical abnormality or gross degeneration was observed. Some osteophytes were observed on the older specimens.

In the first 'preload' test series (Gardner-Morse and Stokes, 2004), there were eight lumbar motion segments (L2-3 and L4-5 from each of four human females, aged 17, 21, 52 and 58 years). See Table 1. These specimens were tested in physiological saline at 4°C . Each specimen was tested with axial compressive preloads of 0, 250 and 500 N (stress approximately 0, 0.15 and 0.3 MPa, comparable with the lower range of physiological values (Wilke et al., 1999)) and was allowed to equilibrate with each preload for at least three hours before each load-displacement test. The six tests (three pure translations and three pure rotations) were sequentially performed with four sawtooth-waveform (ramp-loading) cycles of 87 s (1.15×10^{-2} Hz) in each displacement direction. This loading rate was the slowest possible representing quasi-static conditions, compatible with an acceptable total testing time per specimen (~ 80 h). The applied displacements and resulting forces were recorded at 1 Hz. The displacements were cycles of ± 0.5 mm in anterior-posterior and lateral displacements, ± 0.35 mm axial displacement, ± 1.5 degrees lateral bend rotation and ± 1 degrees flexion-extension and axial rotations. After testing each intact specimen, the facets and ligaments (posterior elements) were removed and the tests were repeated.

In the second 'frequency' tests series (Costi et al., 2008), eight vertebra-disc-vertebra motion segments (posterior elements removed) from seven human lumbar spines (five males, two females, mean [SD] age: 41 [18] years, range: 16–58 years; levels: L1/L2 $n=2$, L2/L3 $n=2$, L3/L4 $n=3$, L4/L5 $n=1$; weight: 84 [19] kg) were tested. According to Thompson's criteria (Thompson et al., 1990) for disc degeneration grade modified for transverse Section, 2 discs were grade 1, 5 were grade 3, and 1 was grade 5. See Table 1. Specimens were loaded with a sine waveform at each of four frequencies (0.001, 0.01, 0.1, and 1 Hz, with displacements and forces recorded at 0.2, 2, 32 and 128 Hz respectively) after equilibration overnight under a preload based on estimated area to produce 0.4 MPa to simulate *in vivo* static loading conditions (Costi et al., 2008). The displacements amplitudes

Table 1
Specimen details for database of lumbar spinal mechanical behavior.

Specimen number	Lumbar level	Disc width (mm)	Disc lateral dimension (mm)	Disc height anterior (mm)	Disc height center (mm)	Disc height posterior (mm)	Disc grade	Donor age (years)	Donor weight (kg)	Gender
Preload Test Series (Specimens tested with and without posterior elements)										
1	L2-3	37.3	49.4	8.4	10.5	5.6		58	122	F
2	L4-5	37.3	51.3	11.2	9.0	4.7		58	122	F
3	L2-3	33.6	42.9	8.4	9.0	3.7		17	52	F
4	L4-5	33.4	44.8	9.4	10.5	4.7		17	52	F
5	L2-3	32.3	42.5	9.4	10.5	4.7		21		F
6	L4-5	32.8	44.0	11.2	11.0	6.5		21		F
7	L2-3	31.6	44.6	9.4	9.0	5.6		52		F
8	L4-5	32.1	46.8	9.4	6.8	4.7		52		F
Mean		33.8	45.8	9.6	9.4	5.0		37.0		
(SD)		(2.3)	(3.1)	(1.1)	(1.4)	(0.8)		(19.4)		
Frequency Test Series (Posterior elements removed)										
1	L1-2	36.5	49.0				3	39	115	F
2	L3-4	41.7	53.1				3	58		M
3	L3-4	44.3	60.9				5	30	102	M
4	L2-3	32.3	42.7				1	19	57	F
5	L2-3	38.2	44.7				3	58	82	M
6	L3-4	44.9	53.7				3	55	77	M
7	L1-2	43.7	50.6				3	55	77	M
8	L4-5						1	16	75	M
Mean		40.2	50.7				2.8	41.3	83.6	
(SD)		(4.2)	(6.1)				(1.3)	(17.7)	(19.1)	

Blank signifies data not available.

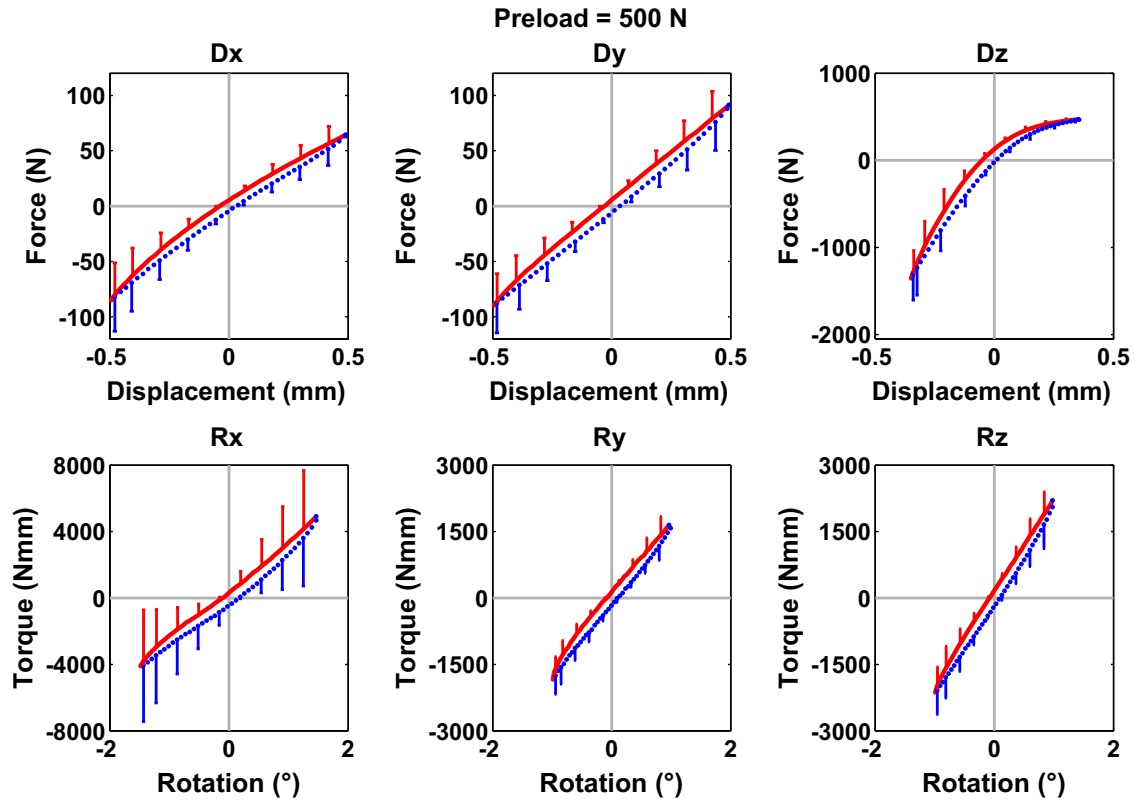


Fig. 1. Illustrative graphs of 'preload' data generated by Matlab[®] code plot_preload.m in the Supplemental data. The graphs for each degree of freedom show the mean and standard deviation (error bars) across specimens of displacement-increasing and displacement-decreasing parts of the recordings of force (or moment) versus displacement (or rotation). Displacement-increasing segments of the tests are shown as solid red lines, and displacement-decreasing segments as dotted blue lines. The preload was 500 N. Positive x, y and z designate anterior, left and superior displacement respectively, with the 'right-hand screw' convention was applied for moments and rotations. (For interpretation of the references to color in this figure legend, the reader is referred to the web version of this article.)

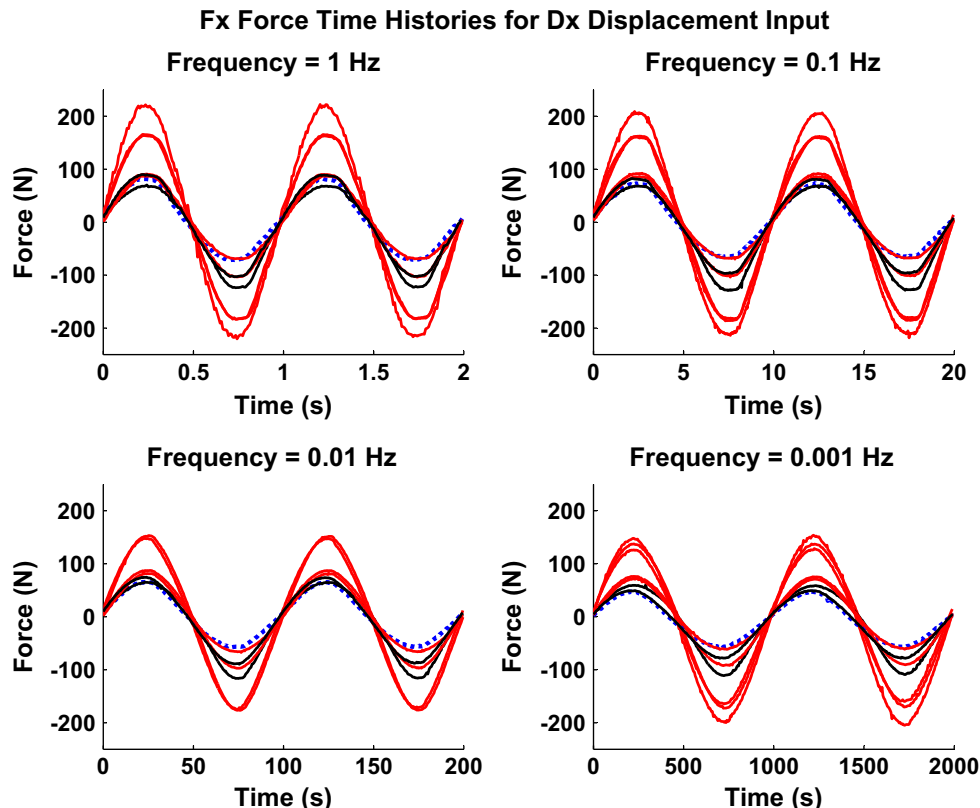


Fig. 2. Illustrative graphs of 'frequency' data generated by Matlab[®] code plot_freq.m in the Supplemental data. Anterior–posterior force F_x was recorded over time at each of four frequencies for all eight specimens under anterior–posterior (Dx) displacement. At each frequency, only the first two cycles of data are presented. Specimen grades are colored as Grade 1: black; Grade 3: red; Grade 5: blue, dotted line (there were no valid data for specimens with Grade 2 or 4 degeneration). (For interpretation of the references to color in this figure legend, the reader is referred to the web version of this article.)

Table 2

Off-diagonal values in stiffness matrices (in units of N, mm and radians) obtained from the preload test series (mean of 8 motion segments). Values are given for three different levels of compressive preloads and for specimens before and after removal of posterior elements. T-tests were used to determine whether each value was statistically equal to zero (*p* values < .05 shown in bold). Also, the complementary off-diagonal values on either side of the matrix diagonal were tested for statistical equality (*p* values > 0.05 shown in bold). The complementary values would be equal for a linear system.

Off-diagonal coupling terms	Facets	Compressive preload (N)	Upper off-diagonal stiffness (K_U)	Lower off-diagonal stiffness (K_L)	$H_0: K_U=0?$ <i>p</i> -value	$H_0: K_L=0?$ <i>p</i> -value	Difference in stiffness	$H_0: K_U=K_L?$ <i>p</i> -value
AP and Lateral Shears	Isolated Discs	0	-0.3	-1.3	0.9173	0.6904	1.0	0.0091
		250	4.7	2.9	0.2316	0.4717	1.8	0.0013
		500	5.0	3.3	0.1984	0.4572	1.6	0.1517
	Intact Motion Segment	0	-8.2	-9.8	0.4490	0.3378	1.7	0.6503
		250	6.6	5.8	0.6052	0.6470	0.8	0.8367
		500	6.9	9.1	0.6055	0.4990	-2.1	0.5972
AP Shears and Compressions	Isolated Discs	0	14.6	6.5	0.3078	0.3786	8.1	0.4334
		250	78.1	93.7	0.0376	0.0677	-15.6	0.3059
		500	119.5	153.1	0.0218	0.0239	-33.6	0.1059
	Intact Motion Segment	0	-10.1	7.8	0.3155	0.5193	-17.9	0.0034
		250	27.2	69.3	0.3750	0.0928	-42.0	0.0110
		500	75.7	140.3	0.0310	0.0150	-64.6	0.0408
AP Shears and Lateral Bendings	Isolated Discs	0	8.8	6.4	0.9041	0.9298	2.4	0.9139
		250	206.5	160.4	0.1107	0.2153	46.1	0.0227
		500	232.1	189.7	0.1501	0.2442	42.4	0.0423
	Intact Motion Segment	0	-79.9	-402.5	0.7690	0.2278	322.6	0.0208
		250	304.7	-40.8	0.3277	0.9170	345.5	0.0593
		500	372.8	-102.0	0.3362	0.8201	474.8	0.0146
AP Shears and Flexion/Extension	Isolated Discs	0	-1,072.7	-1,144.7	0.0000	0.0000	72.0	0.1046
		250	-2,176.8	-2,244.0	0.0000	0.0000	67.2	0.3727
		500	-3,068.9	-3,069.8	0.0000	0.0000	0.9	0.9934
	Intact Motion Segment	0	-6,501.9	-6,525.4	0.0000	0.0000	23.5	0.8914
		250	-9,245.7	-9,266.5	0.0000	0.0000	20.8	0.9648
		500	-9,824.4	-10,287.4	0.0000	0.0000	463.0	0.5005
AP Shears and Axial Rotations	Isolated Discs	0	97.7	134.4	0.1186	0.0094	-36.8	0.1203
		250	162.6	276.3	0.1590	0.0071	-113.8	0.0025
		500	205.4	376.3	0.2019	0.0093	-170.8	0.0007
	Intact Motion Segment	0	228.3	957.8	0.6072	0.0621	-729.5	0.0123
		250	1.3	690.0	0.9978	0.2159	-688.7	0.0102
		500	-10.5	834.2	0.9793	0.1534	-844.7	0.0119
Lateral Shears and Compressions	Isolated Discs	0	-3.5	2.3	0.4293	0.6777	-5.7	0.0774
		250	3.0	12.6	0.8659	0.6077	-9.6	0.2236
		500	0.4	-6.2	0.9853	0.7231	6.6	0.2258
	Intact Motion Segment	0	-3.2	7.7	0.6248	0.1765	-10.9	0.0023
		250	7.4	27.7	0.6780	0.1244	-20.3	0.0165
		500	2.2	23.8	0.9031	0.3120	-21.7	0.0526
Lateral Shears and Lateral Bendings	Isolated Discs	0	1,250.9	1,138.9	0.0000	0.0000	112.1	0.0021
		250	2,901.9	2,931.4	0.0000	0.0000	-29.5	0.7440
		500	3,966.9	4,043.0	0.0000	0.0000	-76.2	0.6124
	Intact Motion Segment	0	6,589.2	7,331.1	0.0000	0.0000	-741.8	0.0033
		250	8,920.0	9,809.1	0.0000	0.0000	-889.1	0.0002
		500	10,264.1	11,713.0	0.0000	0.0000	-1448.9	0.0004
Lateral Shears and Flexion/Extension	Isolated Discs	0	113.7	236.6	0.3019	0.0822	-122.9	0.0345
		250	25.9	277.2	0.6945	0.0273	-251.3	0.0108
		500	-10.0	309.7	0.9074	0.0314	-319.6	0.0034
	Intact Motion Segment	0	420.6	79.7	0.2823	0.8473	341.0	0.2464
		250	124.5	132.5	0.8212	0.8463	-8.0	0.9799
		500	202.0	285.6	0.7248	0.6750	-83.6	0.7652
Lateral Shears and Axial Rotations	Isolated Discs	0	642.8	546.4	0.0007	0.0017	96.4	0.0025
		250	1,278.9	1,055.3	0.0014	0.0040	223.6	0.0004
		500	1,663.3	1,376.1	0.0013	0.0037	287.2	0.0008
	Intact Motion Segment	0	-10,886.3	-11,208.1	0.0000	0.0000	321.8	0.4774
		250	-11,658.0	-12,445.0	0.0000	0.0000	787.0	0.0847
		500	-12,798.8	-14,074.3	0.0000	0.0000	1275.5	0.0165
Compressions and Lateral Bendings	Isolated Discs	0	-106.7	-84.9	0.7006	0.6565	-21.7	0.8609
		250	-602.4	-28.0	0.4856	0.9657	-574.4	0.0640
		500	-737.7	-111.7	0.4495	0.8859	-626.0	0.0747
	Intact Motion Segment	0	-278.7	-298.9	0.3246	0.2645	20.2	0.8441
		250	-308.7	98.0	0.7116	0.8961	-406.7	0.0705
		500	-484.0	357.7	0.6172	0.6990	-841.7	0.0307
Compressions and Flexion/Extension	Isolated Discs	0	-568.8	-395.4	0.0426	0.1632	-173.4	0.2406
		250	132.5	1,326.7	0.8678	0.0620	-1194.1	0.0010
		500	-319.6	1,561.8	0.7568	0.0949	-1881.4	0.0002
	Intact Motion Segment	0	1,015.5	1,722.3	0.1240	0.0000	-706.8	0.0845
		250	2,948.9	5,615.5	0.0037	0.0000	-2666.6	0.0000
		500	3,333.4	7,023.0	0.0601	0.0010	-3689.5	0.0004
Compressions and Axial Rotations	Isolated Discs	0	17.3	-101.1	0.9493	0.6305	118.4	0.4591
		250	-436.3	-71.7	0.5273	0.9034	-364.6	0.0210
		500	-896.9	-169.9	0.3010	0.8100	-727.0	0.0048
	Intact Motion Segment	0	-281.9	-175.4	0.4440	0.6315	-106.6	0.1983
		250	-491.9	-213.5	0.5790	0.8201	-278.4	0.1569

Table 2 (continued)

Off-diagonal coupling terms	Facets	Compressive preload (N)	Upper off-diagonal stiffness (K_U)	Lower off-diagonal stiffness (K_L)	$H_0: K_U=0?$ p-value	$H_0: K_L=0?$ p-value	Difference in stiffness	$H_0: K_U=K_L?$ p-value
Lateral Bendings and Flexion/Extension	Isolated Discs	500	-1,214.6	-636.8	0.2526	0.5516	-577.8	0.0137
		0	1,622.5	3,792.5	0.4083	0.0858	-2170.0	0.1266
		250	-2,805.4	1,307.2	0.4527	0.7260	-4112.6	0.0405
	Intact Motion Segment	500	-5,408.0	1,174.4	0.3243	0.8211	-6582.3	0.0100
		0	13,524.7	3,161.4	0.2571	0.7417	10363.3	0.0518
		250	18,299.2	-4,816.3	0.3325	0.6991	23115.4	0.0231
Lateral Bendings and Axial Rotations	Isolated Discs	500	19,057.2	-4,942.0	0.2829	0.7286	23999.3	0.0063
		0	6,555.8	5,810.3	0.0585	0.1088	745.5	0.0671
		250	20,518.5	19,624.0	0.0162	0.0134	894.5	0.5761
	Intact Motion Segment	500	26,559.8	25,598.6	0.0219	0.0161	961.2	0.7049
		0	-244,875	-224,775	0.0000	0.0000	20,100	0.0298
		250	-259,619	-240,331	0.0000	0.0000	-19288	0.0703
Flexion/Extension and Axial Rotations	Isolated Discs	500	-280,331	-262,861	0.0000	0.0000	-17470	0.0785
		0	3,120.0	-1,742.6	0.1800	0.3687	4862.6	0.0040
		250	6,844.1	-3,631.0	0.0703	0.2821	10475.1	0.0040
	Intact Motion Segment	500	7,402.4	-6,193.3	0.0908	0.1238	13595.7	0.0001
		0	9,747.3	-26,412.8	0.6087	0.1890	36160.1	0.0019
		250	12,523.3	-25,689.2	0.6625	0.3301	38212.5	0.0133
		500	6,287.6	-33,086.6	0.8201	0.2271	39374.3	0.0046

were ± 0.6 mm in anterior–posterior and lateral displacements, ± 0.25 mm axial displacement, ± 3 degrees flexion–extension rotation and ± 2 degrees lateral bend rotation and axial rotation. These specimens were tested immersed in phosphate buffered saline with protease inhibitors at 37 °C, the solution having a pH of 6.8. Total testing time per specimen was ~ 52 h.

For the preload tests, the motion segment coordinate system was centered in the superior vertebral body with the Z-axis joining the centers of the vertebrae and the X and Y coordinates aligned with the anatomical planes as identified on biplanar radiographs (Stokes, et al., 2002) with +X anterior, +Y left and +Z superior. For the frequency tests, the coordinate system was similar but centered in the intervertebral disc. Thus the displacements/rotations were applied and the forces were measured at the center of the disc. The vertebral body center convention was appropriate for generating a stiffness matrix for continuum finite element analyses, whereas the center of the disc convention was appropriate for rigid body kinematics with viscoelastic joints with linear combinations of springs and dashpots (e.g. Maxwell, Kelvin–Voigt and/or standard linear solid models).

For each preload condition in the preload tests, and for the data obtained with and without posterior element, all 36 terms of a stiffness matrix were obtained by least-squares best fit (Matlab[®] 'backslash' operator) to experimental data. The resulting stiffness matrices were then analyzed statistically (by two-tailed *t*-tests) to identify which terms were significantly different from zero and whether pairs of off-diagonal terms expected to be equal by symmetry were equal. Non-zero off-diagonal terms would result from inherent coupling (Goel, 1987) and any experimental axis misalignment relative to the segment's structural axis, while nonlinear behavior would also result in matrix asymmetry. For the data from the frequency tests, the primary terms of the stiffness matrix were obtained by linear regression analysis of recorded displacement–force and rotation–moment data.

3. Results

The dataset, together with sample Matlab[®] programs for reading the files are contained in Supplementary Data. The programs generate the graphical output for the 'preload' data in Fig. 1 and for the 'frequency' data in Fig. 2. Analyses of the 'preload' dataset showed that off-diagonal (coupling) terms were significantly different from zero for all preload conditions and for specimens with and without posterior elements for lateral shear/axial rotation, for anterior shear/flexion–extension and for lateral shear/lateral bending. See Table 2. Anterior shear/flexion–extension and lateral shear/lateral bending coupling terms are 'primary' coupling terms according to Goel (1987). Also, the coupling terms for lateral bend/axial rotation were significantly different from zero in all cases except zero preload without posterior elements. The stiffness matrix for a beam with a rigid anterior–posterior offset also has these four coupling terms plus an additional coupling term between axial displacements and flexion–extension. Beyond these four coupling terms, there were only three cases in which both of the complementary coupling terms were both significantly different from

Table 3

Mean \pm standard deviation (SD) of diagonal stiffness terms of disc specimens without posterior elements. Preload for specimens in the frequency test series was set to 0.4 MPa (mean = 642 ± 132 N). Coordinate directions are x: posterior–anterior shear or lateral bending, y: lateral shear or flexion–extension and z: compression–tension or axial rotation.

Test series	Frequency	Preload		
		0.01	0.0115	
Frequency (Hz)	0.01	0	250	500
Fx/Dx (kN/mm)	0.17 \pm 0.07	0.06 \pm 0.01	0.11 \pm 0.01	0.15 \pm 0.02
Fy/Dy (kN/mm)	0.21 \pm 0.07	0.08 \pm 0.01	0.14 \pm 0.02	0.19 \pm 0.02
Fz/Dz (kN/mm)	3.3 \pm 0.7	0.41 \pm 0.08	1.7 \pm 0.1	2.5 \pm 0.2
Mx/Rx (Nm/deg)	2.8 \pm 2.2	0.92 \pm 0.11	1.9 \pm 0.6	2.7 \pm 0.8
My/Ry (Nm/deg)	2.4 \pm 2.6	0.88 \pm 0.12	1.3 \pm 0.1	1.9 \pm 0.2
Mz/Rz (Nm/deg)	2.4 \pm 1.0	0.85 \pm 0.14	1.7 \pm 0.2	2.2 \pm 0.2

zero. However, there was statistically significant evidence of matrix asymmetry (complementary stiffness terms not equal) in 16 of the 35 cases in which at least one of the coupling terms were significant. For the four significant coupling terms, only nine of the 23 significant cases (39.1%) were not symmetrical and the average asymmetry (calculated as the mean of the absolute values of differences between two values, divided by their average and expressed as a percentage) was 12.5%. See Table 2. Thus, overall, the linearized stiffness matrices included the expected off-diagonal coupling terms, and there was little evidence of additional coupling terms, nor of any substantial degree of matrix asymmetry for the range of input displacements in these tests. Load–displacement behavior was almost linear, except for axial displacement (Dz-direction).

The primary stiffnesses (diagonal terms in the stiffness matrices) were all somewhat smaller than the diagonal stiffness values in the frequency test series for all six degrees of freedom. See Table 3. The differences were probably due to a higher preload (mean 642 N) and possibly due to sex differences (Table 1), differences in the location of the axes center (for rotational degrees of freedom) and/or different dimensional or tissue properties.

4. Discussion

These data provide information for use in validation of finite element models. By including the recordings in all six degrees of freedom

for each principal displacement, they provide complete values of the nonlinear stiffness and hysteresis at any recorded loading condition. A finite element model that reproduces this behavior could then provide information about the state of strain at any location. The stiffening with preload effect is thought to result from the stiffness difference in axial compression (much less stiffness in tension than in compression), probably due to the cable-like properties of collagen fibers in the annulus, together with some large displacement (geometrical) effects (e.g. disc bulge).

Finite element models generally predict that stiffness depends on the state of disc degeneration (Galbusera et al., 2011; Natarajan et al., 2006), supported by some experimental evidence (Zirbel et al., 2013) and on disc dimensions, disc thickness and cross sectional area properties (Chagnon et al., 2010; Meijer et al., 2010; Natarajan and Andersson, 1999; Niemeyer, Wilke and Schmidt, 2012). However, no significant correlations between recorded behavior and dimensions and degeneration state were found by Gardner-Morse and Stokes (2004) and Berkson et al. (1979).

For the relatively small displacements in these experiments, there were few significant unexpected off-diagonal terms and little evidence of significant matrix asymmetry. Assuming testing misalignments are random, statistical tests provided a method to detect significant off-diagonal stiffness terms and significant asymmetries. In comparing the linearized stiffness of the two groups of specimens (Table 3), differences were expected for rotational degrees of freedom since the axis center for the preload tests was at the center of the upper vertebral body while it was at the disc center for the frequency data. Stiffness values in finite element analyses can be transformed to different axis systems by means of a rigid offset.

The variability in the stiffness of these specimens indicates the need for future work to include a greater number of specimens to identify the sources of the variability (age, gender, physical dimensions and state of degeneration, etc.) These relationships in turn should be compared with the predictions made by finite element modeling.

Conflict of interest statement

Both authors do not have any financial and personal relationships with other people or organizations that could inappropriately influence (bias) their work.

Acknowledgments

Data were collected with support from NIH grants R01 44119 and R01 049370.

Appendix A. Supplementary material

Supplementary data associated with this paper can be found in the online version at <http://dx.doi.org/10.1016/j.jbiomech.2016.01.035>.

References

- Berkson, M.H., Nachemson, A.L., Schultz, A.B., 1979. Mechanical properties of human lumbar spine motion segments-Part II: responses in compression and shear; influence of gross morphology. *J. Biomech. Eng.* 101, 53–57.
- Castro, A.P., Wilson, W., Huyghe, J.M., Ito, K., Alves, J.L., 2014. Intervertebral disc creep behavior assessment through an open source finite element solver. *J. Biomech.* 47 (1), 297–301.
- Chagnon, A., Aubin, C.E., Villemure, I., 2010. Biomechanical influence of disk properties on the load transfer of healthy and degenerated disks using a poroelastic finite element model. *J. Biomech. Eng.* 132 (11), 111006.
- Cloyd, J.M., Malhotra, N.R., Weng, L., Chen, W., Mauck, R.L., Elliott, D.M., 2007. Material properties in unconfined compression of human nucleus pulposus, injectable hyaluronic acid-based hydrogels and tissue engineering scaffolds. *Eur. Spine J.* 11, 1892–1898.
- Costi, J.J., Stokes, I.A., Gardner-Morse, M.G., Iatridis, J.C., 2008. Frequency dependent behavior of the intervertebral disc in response to each of six degree of freedom dynamic loading: Solid phase and fluid phase contributions. *Spine* 33 (16), 1731–1738.
- Dreischarf, M., Zander, T., Shirazi-Adl, A., Puttlitz, C.M., Adam, C.J., Chen, C.S., Goel, V.K., Kiapour, A., Kim, Y.H., Labus, K.M., Little, J.P., Park, W.M., Wang, Y.H., Wilke, H.J., Rohlmann, A., Schmidt, H., 2014. Comparison of eight published static finite element models of the intact lumbar spine: predictive power of models improves when combined together. *J. Biomech.* 47 (8), 1757–1766.
- Galbusera, F., Schmidt, H., Noailly, J., Malandrino, A., Lacroix, D., Wilke, H.J., Shirazi-Adl, A., 2011a. Comparison of four methods to simulate swelling in poroelastic finite element models of intervertebral discs. *J. Mech. Behav. Biomed. Mater.* 4 (7), 1234–1241.
- Galbusera, F., Schmidt, H., Neidlinger-Wilke, C., Gottschalk, A., Wilke, H.J., 2011b. The mechanical response of the lumbar spine to different combinations of disc degenerative changes investigated using randomized poroelastic finite element models. *Eur. Spine J.* 20 (4), 563–571.
- Gardner-Morse, M.G., Stokes, I.A.F., 2004. Structural behavior of human lumbar spinal motion segments. *J. Biomech.* 37 (2), 205–212.
- Goel, V.K., 1987. Three-dimensional motion behavior of the human spine – a question of terminology. *J. Biomech. Eng.* 109, 353–355.
- Holsgrove, T.P., Gill, H.S., Miles, A.W., Ghezzi, S., 2015. The dynamic, six-axis stiffness matrix testing of porcine spinal specimens. *Spine J.* 15 (1), 176–184.
- Meijer, G.J., Homminga, J., Hekman, E.E., Veldhuizen, A.G., Verkerke, G.J., 2010. The effect of three-dimensional geometrical changes during adolescent growth on the biomechanics of a spinal motion segment. *J. Biomech.* 43 (8), 1590–1597.
- Natarajan, R.N., Andersson, G.B., 1999. The influence of lumbar disc height and cross-sectional area on the mechanical response of the disc to physiologic loading. *Spine* 24 (18), 1873–1881.
- Natarajan, R.N., Williams, J.R., Andersson, G.B., 2004. Recent advances in analytical modeling of lumbar disc degeneration. *Spine* 29 (23), 2733–2741.
- Natarajan, R.N., Williams, J.R., Andersson, G.B., 2006. Modeling changes in intervertebral disc mechanics with degeneration. *J. Bone Jt. Surg.* 88 (Suppl. 2), S36–S40.
- Niemeyer, F., Wilke, H.J., Schmidt, H., 2012. Geometry strongly influences the response of numerical models of the lumbar spine – a probabilistic finite element analysis. *J. Biomech.* 45 (8), 1414–1423.
- O'Connell, G.D., Sen, S., Elliott, D.M., 2012. Human annulus fibrosus material properties from biaxial testing and constitutive modeling are altered with degeneration. *Biomech. Model. Mechanobiol.* 11 (3–4), 493–503.
- Qasim, M., Natarajan, R.N., An, H.S., Andersson, G.B., 2012. Initiation and progression of mechanical damage in the intervertebral disc under cyclic loading using continuum damage mechanics methodology: a finite element study. *J. Biomech.* 45 (11), 1934–1940.
- Schmidt, H., Galbusera, F., Rohlmann, A., Shirazi-Adl, A., 2013. What have we learned from finite element model studies of lumbar intervertebral discs in the past four decades? *J. Biomech.* 46 (14), 2342–2355.
- Schmidt, H., Shirazi-Adl, A., Galbusera, F., Wilke, H.J., 2010. Response analysis of the lumbar spine during regular daily activities – a finite element analysis. *J. Biomech.* 43 (10), 1849–1856.
- Schroeder, Y., Huyghe, J.M., van Donkelaar, C.C., Ito, K., 2010. A biochemical/biophysical 3D FE intervertebral disc model. *Biomech. Model. Mechanobiol.* 9, 641–650.
- Stokes, I.A.F., Gardner-Morse, M., Churchill, D., Laible, J.P., 2002. Measurement of a spinal motion segment stiffness matrix. *J. Biomech.* 35, 517–521.
- Thompson, J.P., Pearce, R.H., Schechter, M.T., et al., 1990. Preliminary evaluation of a scheme for grading the gross morphology of the human intervertebral disc. *Spine* 15, 411–415.
- Wagnac, E., Arnoux, P.J., Garo, A., El-Rich, M., Aubin, C.E., 2011. Calibration of hyperelastic material properties of the human lumbar intervertebral disc under fast dynamic compressive loads. *J. Biomech. Eng.* 133 (10), 101007.
- Weisse, B., Aiyangar, A.K., Affolter, Ch, Gander, R., Terrasi, G.P., Ploeg, H., 2012. Determination of the translational and rotational stiffnesses of an L4–L5 functional spinal unit using a specimen-specific finite element model. *J. Mech. Behav. Biomed. Mater.* 13, 45–61.
- Wilke, H.J., Neef, P., Caimi, M., Hoogland, T., Claes, L.E., 1999. New in vivo measurements of pressures in the intervertebral disc in daily life. *Spine* 24 (8), 755–762.
- Zhang, Q.H., Teo, E.C., 2008. Finite element application in implant research for treatment of lumbar degenerative disc disease. *Med. Eng. Phys.* 30 (10), 1246–1256.
- Zirbel, S.A., Stolworthy, D.K., Howell, L.L., Bowden, A.E., 2013. Intervertebral disc degeneration alters lumbar spine segmental stiffness in all modes of loading under a compressive follower load. *Spine J.* 13 (9), 1134–1147.